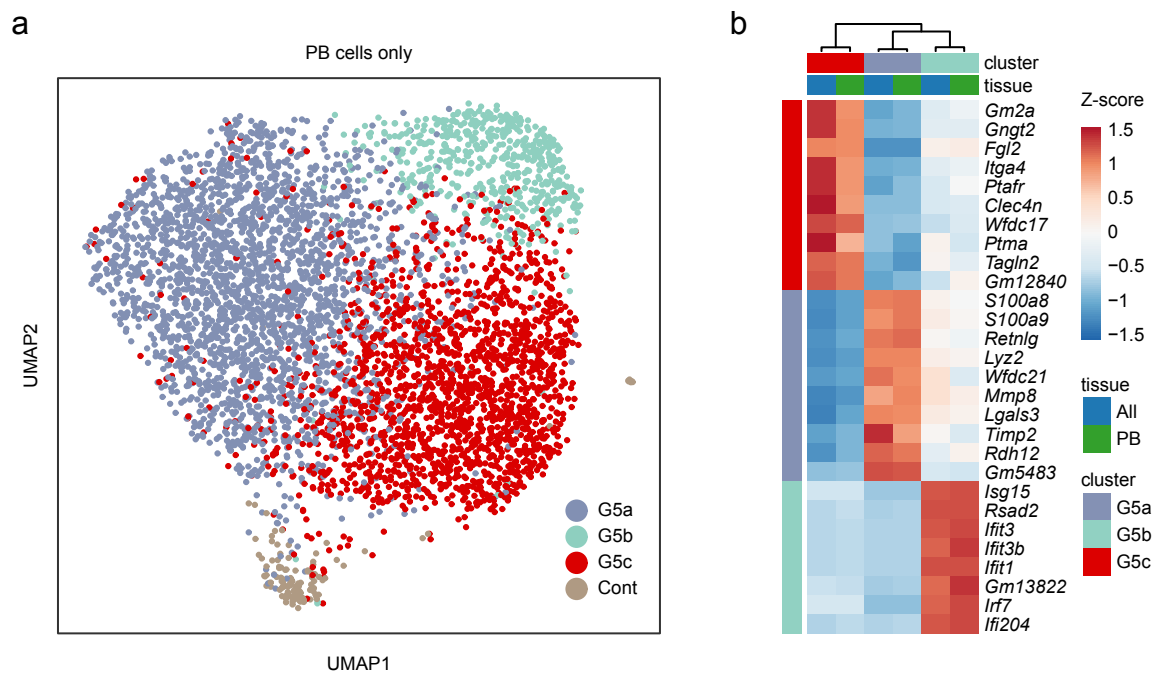
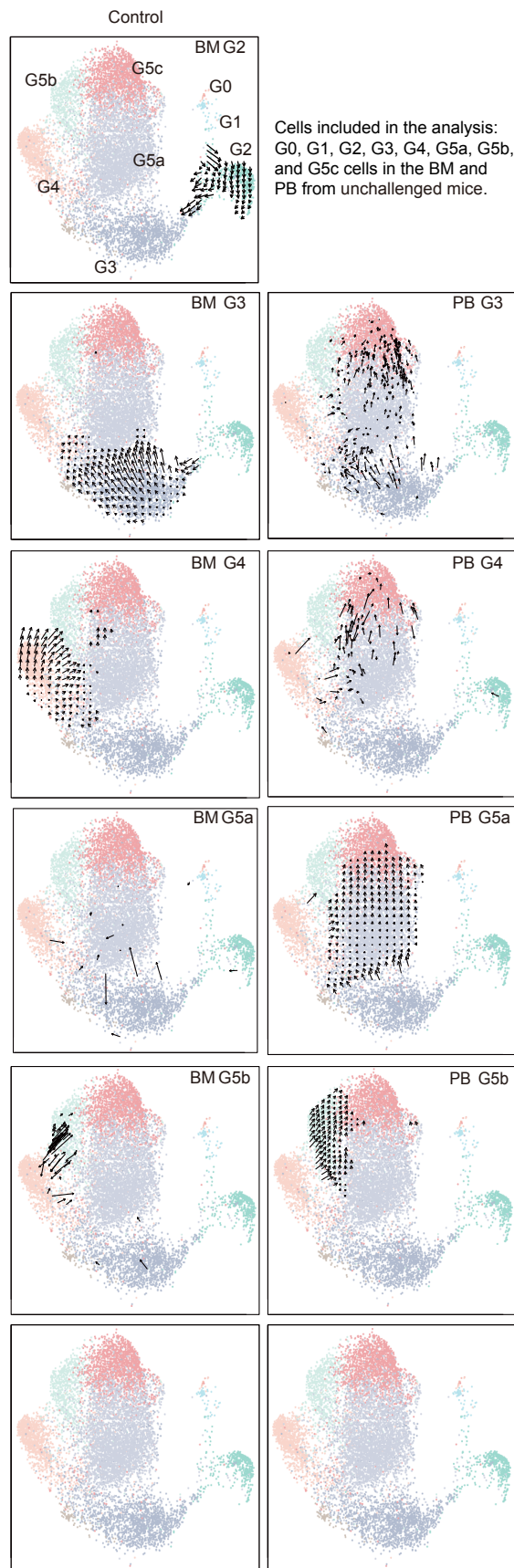


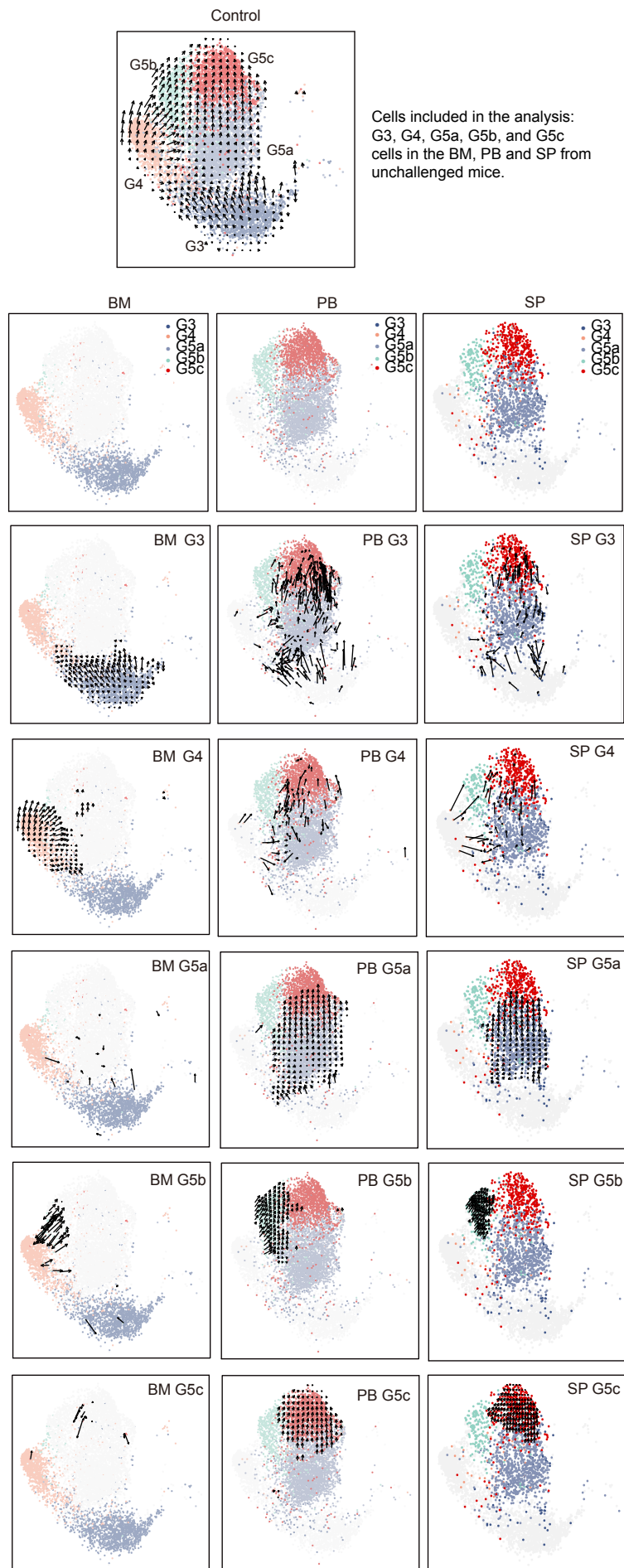
Supplementary Fig. 1. scRNA-seq defined differentiating neutrophil populations correlated with classical morphology-defined neutrophil subpopulations. (a) Heatmaps showing row-scaled expression of the 20 highest DEGs per cluster across averaged single-cell groups (left) and morphological groups (right). Only genes detected in both scRNA-seq data and bulk RNA-seq data are visualized. Representative genes are indicated. **(b,c)** Heatmaps showing row-scaled expression of granule-related genes (b) and cell-cycle related genes (c) for morphological groups.



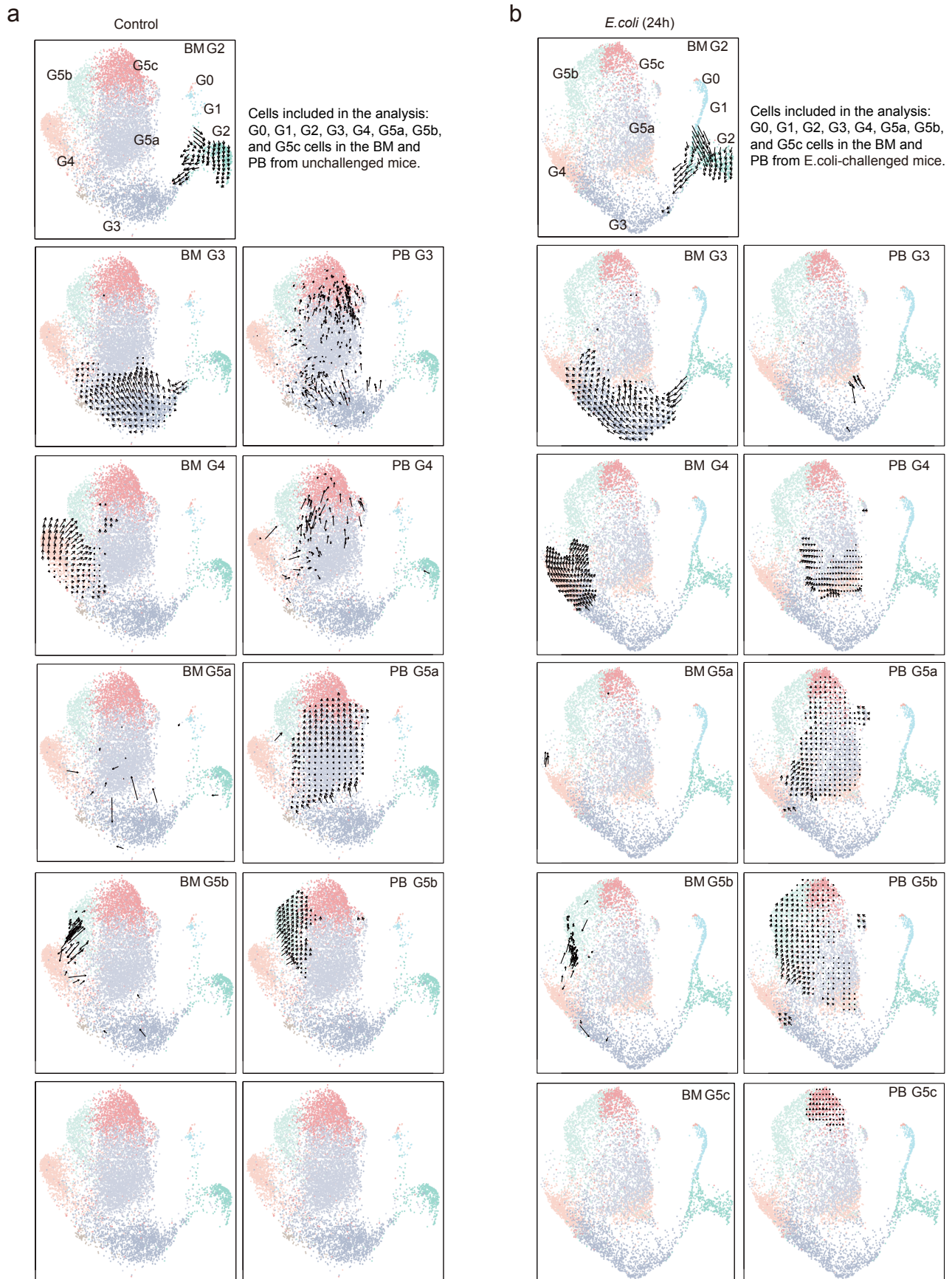
Supplementary Fig. 2. Clustering of PB neutrophils only gave rise to the same three G5 subpopulations. (a) UMAP of mouse PB neutrophils only. Cells were colored by their de novo-defined identity. **(b)** Heatmap showing row-scaled expression of the 10 highest differentially expressed genes (Fig. 2g) in G5 clusters defined in Fig. 1b (All) and in (a) (PB).



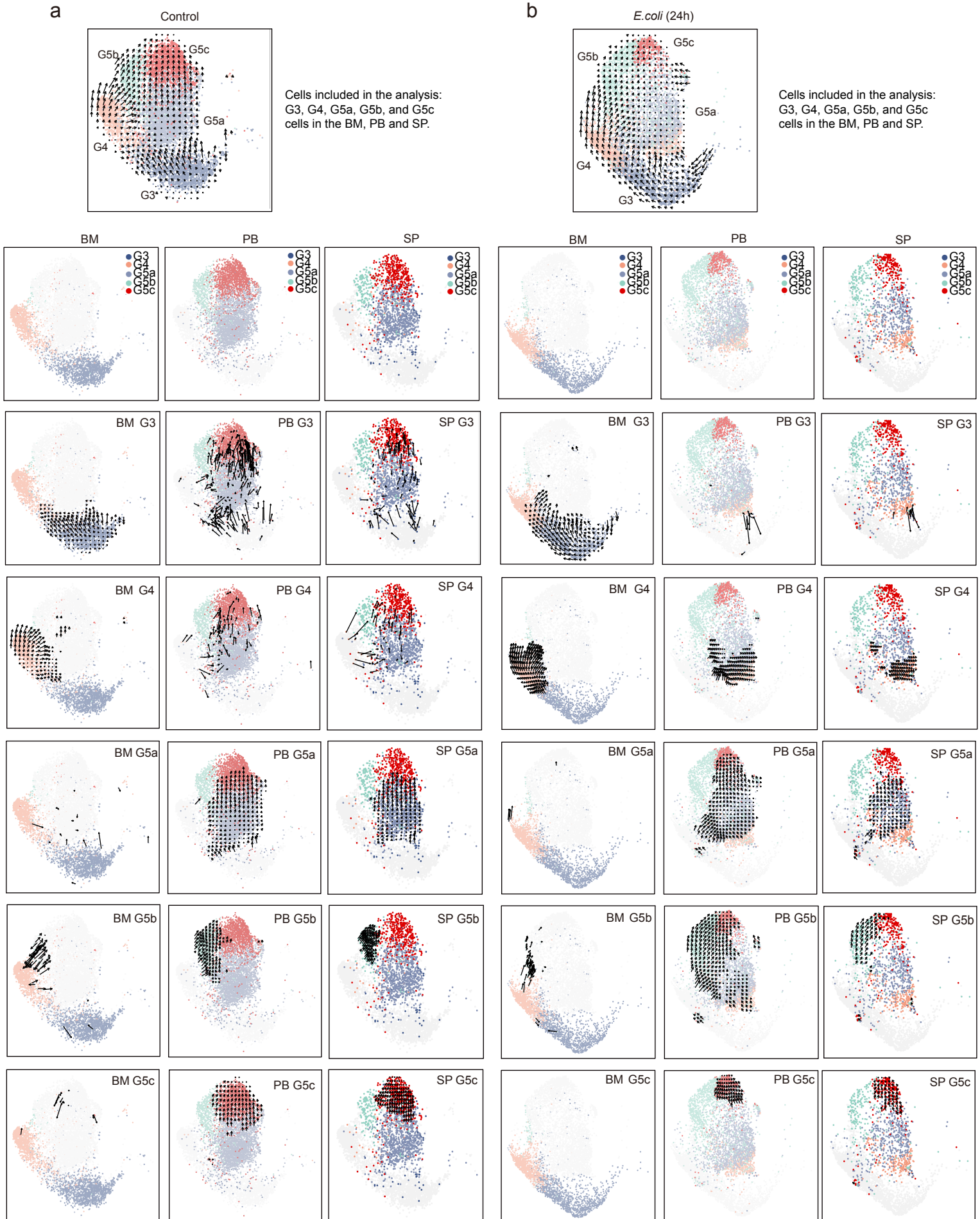
Supplementary Fig. 3. Neutrophil dynamics under steady-state assessed by velocity analysis (all neutrophil populations were included for analysis). Shown are dynamics (velocity field projected on the UMAP plot) of G2-G5 neutrophils under normal conditions. BM neutrophils (left) and PB neutrophils (right) are displayed separately. For small populations, velocity vectors of all cells are visualized directly. For large populations, a grid velocity summary is derived by calculating the Gaussian-weighted average of velocity vectors of all cells at each grid point. Only grid points adjacent to neutrophils in the target population are visualized..



Supplementary Fig. 4. Neutrophil dynamics under steady-state assessed by velocity analysis (Only G3-G5 neutrophil populations were included for analysis). The RNA velocity analysis was conducted as described in supplementary Fig. 3. Only G3-G5 neutrophils from BM-Gr1+, PB-Gr1+, and SP-Gr1+ samples were utilized for the analysis.

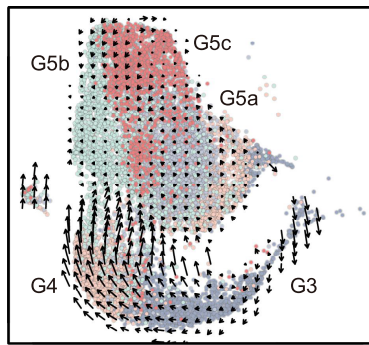


Supplementary Fig. 5. Neutrophil dynamics under steady-state and bacterial infection conditions assessed by velocity analysis (all neutrophil populations were included for analysis). The analysis was conducted as described in Supplementary Fig. 3.

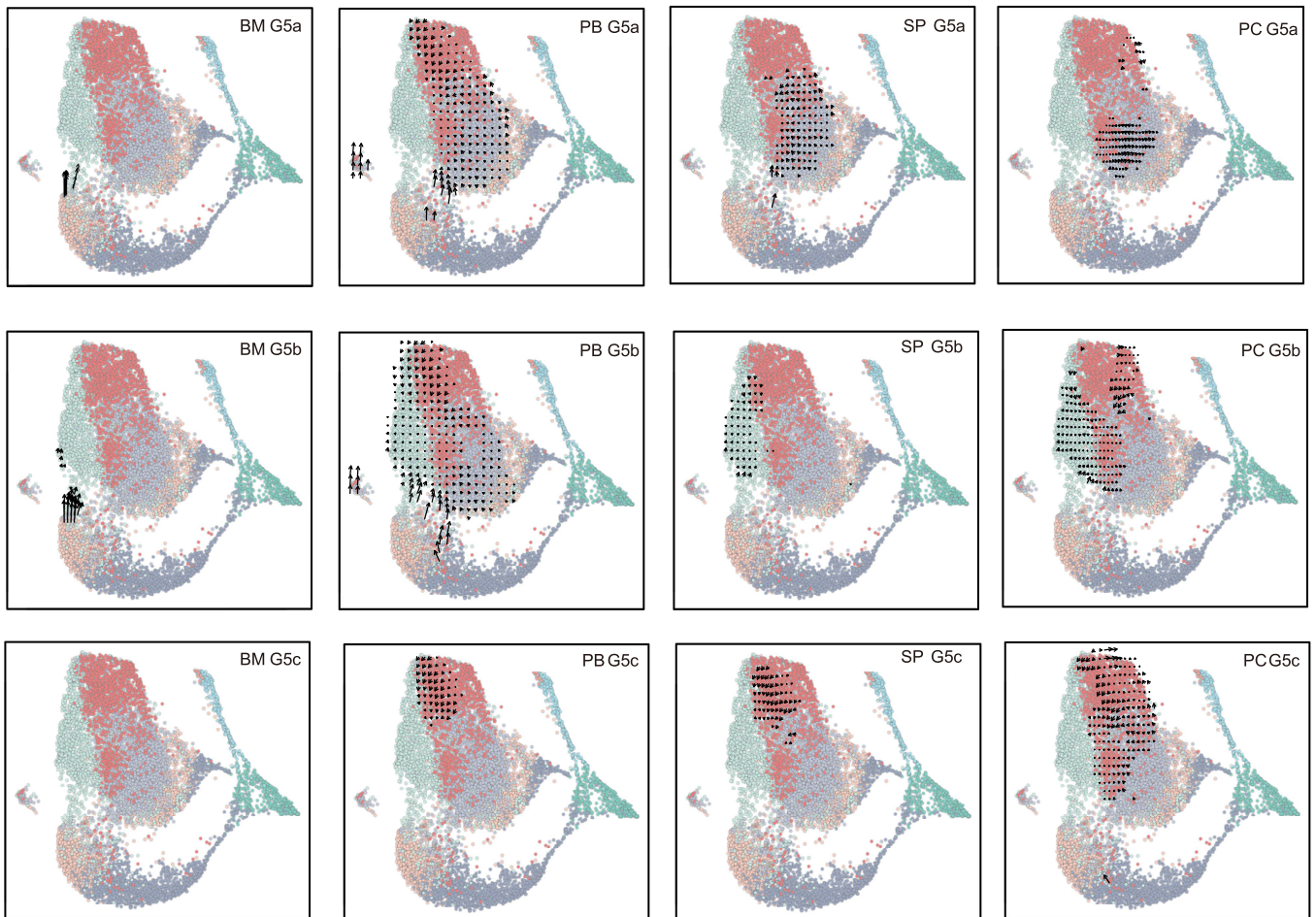


Supplementary Fig. 6. Neutrophil dynamics under steady-state and bacterial infection conditions assessed by velocity analysis (only G3-G5 neutrophil populations were included for analysis).
The analysis was conducted as described in Supplementary Fig. 4.

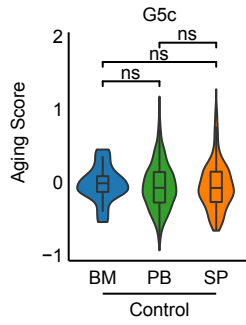
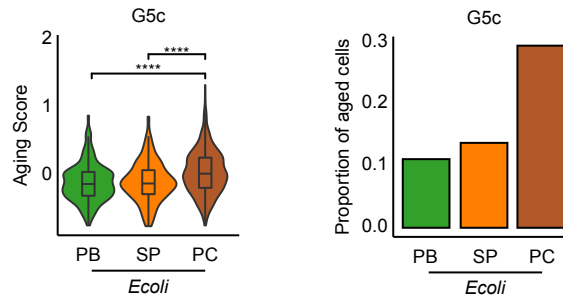
E.coli (24h)



Cells included in the analysis:
G3, G4, G5a, G5b, and G5c
cells in the BM, PB, SP and PC.



Supplementary Fig. 7. Dynamics of G5 neutrophils during bacterial infection assessed by velocity analysis. G3-G5 neutrophils from BM-Gr1+, PB-Gr1+, SP-Gr1+ and PC-Gr1+ samples (*E.coli* challenged) were subjected to RNA velocity analysis. Upper: Velocity analysis revealing the origin and inter-relationship of neutrophil subpopulations. Velocity fields were projected onto the UMAP plot. Lower: Visualization of RNA velocity analysis results. G5 subpopulations in the BM, PB, SP and PC are displayed separately.

a**b**

Supplementary Fig. 8. Organ specific aging property of G5c neutrophils. (a) Violin plot of aging score defined as weighted average Z-scores of aging-related genes for control (unchallenged) G5c neutrophils across organs. **(b)** Left: Violin plot of aging score defined as weighted average Z-scores of aging-related genes for *E. coli*-challenged G5c neutrophils across organs. Right: Proportion of aged cells in G5c population across organs. ns, $P > 0.05$; *, $P \leq 0.05$; **, $P \leq 0.01$; ***, $P < 0.001$, ****, $P \leq 0.0001$. Student's t-test.